



Published in final edited form as:

Med Phys. 2017 July ; 44(7): 3848–3860. doi:10.1002/mp.12339.

A Monte Carlo model for mean glandular dose evaluation in spot compression mammography

Antonio Sarno^{1,2}, David R. Dance^{3,4}, Ruben E. van Engen⁵, Kenneth C. Young^{3,4}, Paolo Russo^{1,2}, Francesca Di Lillo^{1,2}, Giovanni Mettivier^{1,2}, Kristina Bliznakova⁶, Baowei Fei^{7,8}, and Ioannis Sechopoulos^{5,9}

¹Università di Napoli Federico II, Dipartimento di Fisica “Ettore Pancini”, Via Cintia, I-80126 Napoli, Italy ²INFN Sezione di Napoli, I-80126 Napoli, Italy ³National Co-ordinating Centre for the Physics of Mammography (NCCPM), Royal Surrey County Hospital, Guildford GU2 7XX, United Kingdom ⁴Department of Physics, University of Surrey, Guildford, GU2 7XH, United Kingdom ⁵Dutch Reference Centre for Screening (LRCB), PO Box 6873, 6503 GJ Nijmegen, The Netherlands ⁶Department of Electronics, Technical University of Varna, 1 Studentska Str, Varna, 9010 Bulgaria ⁷Department of Radiology and Imaging Sciences, Emory University School of Medicine, 1701 Upper Gate Drive Northeast, Suite 5018, Atlanta, Georgia 30322, USA ⁸Department of Biomedical Engineering, Emory University and Georgia Institute of Technology, Atlanta, Georgia 30322, USA ⁹Department of Radiology and Nuclear Medicine, Radboud University Medical Centre, P.O. Box 9101, 6500 HB Nijmegen, The Netherlands

Abstract

Purpose—To characterize the dependence of normalized glandular dose (DgN) on various breast model and image acquisition parameters during spot compression mammography and other partial breast irradiation conditions, and evaluate alternative previously-proposed dose-related metrics for this breast imaging modality.

Methods—Using Monte Carlo simulations with both simple homogeneous breast models and patient-specific breasts, three different dose related metrics for spot compression mammography were compared: the standard DgN, the normalized glandular dose to only the directly irradiated portion of the breast (DgN_v), and the DgN obtained by the product of the DgN for full field irradiation and the ratio of the mid-height area of the irradiated breast to the entire breast area (DgN_M). How these metrics vary with field-of-view size, spot area thickness, x-ray energy, spot area and position, breast shape and size, and system geometry was characterized for the simple breast model and a comparison of the simple model results to those with patient-specific breasts was also performed.

Results—DgN in spot compression mammography can vary considerably with breast area. However, the difference in breast thickness between the spot compressed area and the

Corresponding author: Ioannis Sechopoulos, PhD, DABR, ioannis.sechopoulos@radboudumc.nl, Radboud university medical center, P.O. Box 9101, 6500 HB Nijmegen (766), The Netherlands.

Financial disclosures: IS has research and speaking agreements with Siemens Healthcare, and is a member of the Scientific Advisory Board of Fischer Medical.

uncompressed area does not introduce a variation in DgN . As long as the spot compressed area is completely within the breast area and only the compressed breast portion is directly irradiated, its position and size does not introduce a variation in DgN for the homogeneous breast model. As expected, DgN is lower than DgN_v for all partial breast irradiation areas, especially when considering spot compression areas within the clinically used range. DgN_M underestimates DgN by 6.7% for a W/Rh spectrum at 28 kVp and for a 9×9 cm² compression paddle.

Conclusion—As part of the development of a new breast dosimetry model, a task undertaken by the American Association of Physicists in Medicine and the European Federation of Organizations of Medical Physics, these results provide insight on how DgN and two alternative dose metrics behave with various image acquisition and model parameters.

Keywords

mammography; spot compression; magnification mammography; mean glandular dose

1. Introduction

Several authors have performed Monte Carlo (MC) simulations to compute the normalised glandular dose conversion coefficients (DgN) which are used to estimate mean dose to the glandular component of the breast tissue (mean glandular dose – MGD) during full field mammography from measurements of the incident air kerma or exposure^{1–9}. In these studies, the breast has been modelled as a homogeneous mixture of adipose and glandular tissue surrounded by a shielding layer which simulates either a 0.4 cm thick layer of skin or a 0.5 cm thick layer of adipose tissue. It is fully irradiated, and the MGD is assumed independent of the source to breast distance and of the breast diameter.

Spot compression mammography is routinely used during diagnostic work-up of screening or clinical findings. This work aims at investigating, via MC simulations, the effects of model parameters (breast diameter, shape of the compressed breast, distance between the source and the breast, position of the irradiated area) on the estimates of glandular dose to the breast in spot compression mammography with particular interest in the cases in which only a part of the breast is directly irradiated. In addition, results obtained with homogeneous breast models (where the breast is simulated as a homogeneous mixture of glandular and adipose tissue surrounded by a skin layer) have been compared to those obtained using breast models with realistic glandular tissue distributions developed from breast CT images. It is not the aim of this work to determine the normalized glandular dose coefficients for all acquisition conditions and systems from different manufacturers. That task will be performed in the future by a joint task group of the American Association of Physicists in Medicine (AAPM)²⁴ and the European Federation of Organizations for Medical Physics (EFOMP) based, in part, on the results of this study.

2. Materials and methods

2.A. Dosimetric parameters

In the case of partial volume irradiation, one has to take into account the energy (E_V) absorbed in the directly irradiated glandular breast mass (M_V) as well as the energy

absorbed in the indirectly irradiated portion of the breast (E_S) due to scattered photons. Hence, the MGD (the ratio between the total energy absorbed in the glandular tissue, E_T , and the total mass of the glandular tissue, M_T) is defined as:

$$\text{MGD} = \frac{E_T}{M_T} = \frac{E_S + E_V}{M_T} \quad (1)$$

Mettivier *et al*¹⁰, in their investigation of partial irradiation of the breast with a thin laminar beam from a synchrotron radiation source, defined the quantity:

$$\text{MGD}_V = \frac{E_V}{M_V} \quad (2)$$

In this case, only the glandular mass directly irradiated is taken into account, leading to larger dose values than those obtained with eq. 1, in particular for irradiation of small volumes¹⁰. The concept of MGD_V expressed by eq. 2 was introduced for the first time for the partial breast irradiation in magnification mammography by Liu *et al*¹¹ and investigated by Koutaloni *et al*¹².

An approximate method of estimating MGD for magnification view spot compression has been proposed in Report 89 of IPEM¹³, and is used in the United Kingdom and in Germany, and has been also included in this study. This approximation is denoted MGD_M and is defined as:

$$\text{MGD}_M = \frac{E_{FF}}{M_T} \times \frac{A_I}{A_F} \quad (3)$$

where E_{FF} is the energy absorbed for a full-field irradiation, M_T is as defined for eq. 1, A_I is the directly irradiated area at the mid-plane of the breast and A_F is the area of the compressed breast¹³. For the present calculation A_F has been taken as 226.2 cm², the area of a compressed breast modeled as a cylinder with a semi-circular cross section with a radius of 12 cm (see below). This approximation involves the use of the conventional full-field estimate of MGD. It permits the use of commonly-adopted whole-breast MGD estimates and avoids the calculation of new DgN coefficients, since the MGD in spot mammography would be obtained by simply calculating the ratio of the irradiated area to the whole breast area. Use of MGD_M in place of MGD assumes that any energy deposition events occurring outside the directly irradiated tissue volume are negligible. In this study we aim to determine what is the error introduced, if any, by using this simplification.

For each definition, the normalized glandular dose coefficients (DgN, DgN_V , and DgN_M , in mGy/mGy) are evaluated by dividing the values of the respective absorbed doses in eqs. 1–3 by the incident air kerma (K) at the entrance skin surface.

2.B. Breast models

2.B.1. Homogenous breast model—In the homogeneous model developed in the USA^{2,3}, the breast is simulated as a cylinder with a semi-elliptical cross section composed of a homogeneous mixture of glandular and adipose tissue, surrounded by a 0.4-cm skin layer. The composition of the breast tissues is that proposed by Hammerstein *et al*⁴. During spot compression the uncompressed area of the breast is thicker than the compressed area. In this work, a breast model with a constant thickness as used by Liu *et al*¹¹ and Koutaloni *et al*¹² in partial breast irradiation, named the “full homogeneous phantom” (fig. 1a), has been compared to a model which considers a thicker portion of the breast for the uncompressed area with respect to the spot area, named the “spot homogeneous phantom”. For this, a rectangular block was subtracted from the full-field compressed breast to mimic the thinner portion of the breast experiencing the spot compression (fig. 1b). In order to evaluate the influence of the breast shape on the absorbed energy, various spot homogeneous breast phantoms were modelled with a constant thickness of 3 cm between the compression paddle and breast support table, while varying the uncompressed breast thickness between 3 cm (constant compression thickness) and 7 cm. The breast radius was modified so as to maintain a constant total glandular mass in all cases. In the case of the uncompressed breast thickness of 3 cm a breast radius of 12 cm was adopted.

To study the influence of breast diameter on the glandular dose estimates, the radius was varied between 9 cm and 15 cm (compressed breast thickness = 3 cm; uncompressed breast thickness = 6 cm). In the case of DgN_M , E_{FF} was always calculated for a standard breast with a radius of 12 cm. In this work, the breast was modeled as a cylinder with semi-circular cross section, differently from the semi-elliptical cross section adopted in the USA standard².

2.B.2. Patient specific phantoms—In this work, the patient specific phantoms developed by Sechopoulos *et al*¹⁵ were used to characterize the difference between dose estimates using the homogeneous simple model breast and patient specific phantoms. Briefly, Sechopoulos *et al*¹⁵ used images obtained from dedicated breast CT clinical scans of 20 different breasts to construct voxel phantoms of the pendant breast as imaged in CT. The voxels were classified into four categories: air, skin, adipose and glandular tissue¹⁶ and the phantoms compressed as for a cranio-caudal (CC) mammographic acquisition¹⁷. Table I shows the mean value, the minimum, the maximum and the standard deviation of the compressed breast thickness, the area and the glandular fraction by mass (skin excluded) of the 20 breasts. The software developed for mimicking the breast compression produces only fully compressed breasts (fig. 2a), named the “full heterogeneous phantom”. In order to simulate spot compression, the upper portion of each fully compressed breast (summarized in Table I) was cut out to obtain a breast with a portion compressed to 60% of the thickness of the breast undergoing full field compression (fig. 2b), named the “spot heterogeneous phantom”.

In order to study the variation in dose with breast geometry, the difference in thickness between the compressed and uncompressed portions of the spot heterogeneous phantom was varied as shown in figs. 2b, 2c and 2d. To maintain a constant overall glandular mass when

the uncompressed portion of the breast thickness was varied, the increase in glandular mass in the additional uncompressed portion was compensated by removing a portion of breast tissue from the outer part of the breast phantom. Where necessary to ensure a complete layer, a 2.184 mm thick layer of skin (8 voxels) was added, which is the average skin thickness at the upper surface of the 20 3D breast images after compression.

2.C. Irradiation geometry

In our MC simulations, x-rays were emitted isotropically from a point source located 43.3 cm from the breast support table and, apart from the cases considered in section 2.G, the x-ray beam was collimated to irradiate a surface at the breast support table as large as the compression paddle. The heel effect was not included in the simulation of the x-ray source, since up to now it is not included in the commonly used breast dosimetry models^{1–8}. This approximation has been found to introduce a variation of up to 7% in the DgN in full field mammography.¹⁸ Therefore, the variation in spot compression and partial breast irradiation should be even smaller, due to the more limited x-ray field area used in these techniques.

In additional simulations, the effect of varying the distance between the breast support table and the source was evaluated in the range 34.3–64.5 cm, for 5 cm breast thickness, 20% glandular fraction by mass and W/Rh spectrum. Figure 3 shows the irradiation geometry. The distance 64.5 cm corresponded to spot compression with the breast on the standard support used for full field mammography.

The compression paddle and breast support table were in all simulations represented as 0.2 cm thick polymethyl-methacrylate (PMMA) sheets. The breast support table had an area of $14 \times 26 \text{ cm}^2$ while the compression paddle had an area of $9 \times 9 \text{ cm}^2$, which is the compression paddle used by the clinical system at our institution (MAMMOMAT Innovation, Siemens Healthineers, Forchheim, Germany)¹, as well as being a paddle available with most other mammographic systems. Since many other shapes and dimensions of compression paddles are available, the dimensions of the square compression paddle were varied between $1 \times 1 \text{ cm}^2$ and $14 \times 14 \text{ cm}^2$, in addition to the full-field irradiation with a $14 \times 26 \text{ cm}^2$ compression paddle, in order to investigate the impact of paddle area on dose. Moreover, the variation in results when using a D-shaped compression paddle was investigated (see Section 2.G).

Throughout the manuscript, the sizes of the directly irradiated fields are given as the x-ray field size at the bottom of the breast, i.e. at the breast support table. For this, for compression paddle areas between $1 \times 1 \text{ cm}^2$ and $10 \times 10 \text{ cm}^2$, the directly irradiated breast area is calculated by multiplying the paddle area by the square of the source-to-breast surface entrance distance to the source-to-support table distance ratio. However, for the paddle with area $14 \times 14 \text{ cm}^2$, which extends beyond the breast surface, a more complex calculation is needed, and for simplicity, we just report its value to be 141.7 cm^2 . In similar fashion, for full field irradiation (paddle area $14 \times 26 \text{ cm}^2$), the area is reported as 226.2 cm^2 .

¹<http://www.deltamedicalsystems.com/DeltaMedicalSystems/media/Product-Details/Tomo-Data-Sheet.pdf>, accessed on 03-01-2017

In its standard position the paddle was centred laterally (y direction) and with its centre 4.5 cm anterior to the chest wall (+x direction). In order to investigate the influence of compression paddle position on dose, its position along the centre line of the breast was varied so that the distance along the +x-direction between it and the chest-wall was in the range of 0–5 cm. Lateral (y-direction) displacement of the paddle was also investigated with the distance between the centre of the paddle and the centre line of the breast varied in the range of 0–7 cm. In all cases, the distance between detector and source was 65.5 cm. To take into account any backscatter, the patient body was modeled as a water box of volume $30 \times 30 \times 17 \text{ cm}^3$.

2.D. Monte Carlo simulations

MC simulations were performed with the GEANT4 toolkit version 10.00, including the electromagnetic physics list option 4 package. Photoelectric interactions, incoherent and coherent scattering were simulated; the electrons were not tracked but assumed to deposit their energy locally at the point of x-ray interaction. The default cut range for photons was used (1 mm, corresponding to an energy of 2.5 keV in 20% glandular breast tissue). The dose absorbed in the breast tissue was evaluated using:

$$\text{Glandular dose} = \frac{\sum_i G_i(E) \times E_i^{\text{dep}}}{f_g \times W_b} \quad (4)$$

where f_g is the breast glandular fraction by mass, W_b is the breast mass without considering the skin in the considered volume (total or directly irradiated), and E_i^{dep} is the energy deposited by the incident photon or by the electron at the i -th interaction in the considered volume. $G_i(E)$ was evaluated using:

$$G(E) = \frac{f_g \times \frac{\mu_{\text{en}}}{\rho}(E)_g}{f_g \times \frac{\mu_{\text{en}}}{\rho}(E)_g + (1 - f_g) \times \frac{\mu_{\text{en}}}{\rho}(E)_a} \quad (5)$$

where μ_{en}/ρ is the mass energy absorption coefficient of glandular (subscript g) and adipose (subscript a) tissues, evaluated by considering the functional interpolation given by Fedon *et al*¹⁹. The factor G was evaluated at energy E of the photon which deposits energy or, in case of the electron energy loss, at the energy of the photon which generated such an electron through a photoelectric or incoherent interaction. K was evaluated under the compression paddle, in a square region of interest (S) of area $0.8 \times 0.8 \text{ cm}^2$ at the entrance breast skin surface attached to the chest-wall using:

$$K = \sum_i \frac{E_i \times \frac{\mu_{\text{en}}}{\rho}(E_i)_{\text{air}}}{S \times \cos\theta_i} \quad (6)$$

here E_i is the photon energy of the i -th photon crossing the scoring surface, $\mu_{\text{en}}/\rho(E_i)_{\text{air}}$ is the mass energy absorption coefficient of dry air²⁰ and θ_i is the angle between the photon

direction and the vector normal to the scoring plane. In the evaluation of K , both primary radiation and scatter from the compression paddle were taken into account, but backscatter from the breast was not included.

Simulations with monoenergetic x-ray beams were performed with photons in the energy range of 8–45 keV. Polyenergetic normalized glandular dose coefficients were evaluated for a W/Rh (Rh filter thickness of 0.050 mm) mammographic spectrum at 28 kVp (1st HVL below 0.2 cm PMMA compression paddle = 0.511 mm Al) modeled following Hernandez *et al*²¹. The statistical uncertainty achieved in all simulations was below 0.2%.

2.E. Monte Carlo validation

The MC code developed for the homogeneous model was previously validated as suggested by the AAPM Report TG195²², cases 1–3²³. As shown in that publication, the results obtained with our code for case 3 of the Report, which simulated the MGD to the breast during a mammographic examination, are within 0.5% of those provided by the Report, therefore within the statistical uncertainty of the results (0.2% in the case of TG195 and 0.4% with our code²³).

In the case of simulations with voxelised breasts, two validation tests were performed. First, the code was also validated against the AAPM – TG195 Report case 3²². For this comparison, the Report geometry was replicated, but with the breast represented as a voxelised breast of semi-circular cross section with a voxel size of $0.5 \times 0.5 \times 0.5 \text{ mm}^3$. All voxels representing breast tissue, excluding skin, were composed of a homogeneous mixture of adipose and glandular tissue with the appropriate glandular fraction. The results of this simulation were directly compared to those included in the AAPM TG 195 Report.

As a second validation of simulations with voxelised breasts, a set of 10 heterogeneous breasts was created by randomly assigning each voxel representing breast tissue as either fully glandular or adipose voxels. The number of glandular voxels (v_g) in each phantom was set according to:

$$v_g = \frac{f_g \times \rho_a}{(1 - f_g) \times \rho_g + f_g \times \rho_a} \times V \quad (7)$$

where ρ_a and ρ_g are, respectively, the densities of adipose and glandular tissue according to Hammerstein *et al*¹⁴, V is the total number of voxels in the breast model (excluding the skin) and f_g is the glandular fraction. The MC simulation results obtained with the 10 different phantom realizations were averaged and compared to the results of using the homogeneous breast model as described in sect. 2.B.1 (breast diameter = 12 cm, full-field breast compression, breast thickness = 5 cm, glandular fraction = 20%, compression paddle dimension = $9 \times 9 \text{ cm}^2$, source to breast support distance = 43.3 cm). In these simulations the voxel size was set to $0.5 \times 0.5 \times 0.5 \text{ mm}^3$. The simulations were performed for W/Rh spectra and tube voltage ranging between 18 kVp and 40 kVp.

2.F. Homogeneous breast model vs. patient specific dosimetry

In order to compare the dosimetry of the homogeneous breast model to the more realistic patient specific phantoms, we calculated DgN and DgN_V coefficients for the full homogeneous breast model described in sect. 2.B.1 and for the patient specific full heterogeneous phantoms shown in fig. 2a. This version of the patient model, as opposed to the spot phantoms were used to avoid introducing artificial glandular tissue distributions due to the removal of the upper portion of the breast representation in the heterogeneous phantoms, resulting in the densest portion of the breasts being located adjacent to the x-ray incident surface of the breast. For the homogeneous breast we used a breast thickness range of 2–8 cm (in 1 cm steps) and glandular fractions of 6%, 12%, 23.1% (i.e. the mean value from Table 1), 32% and 42% in the case of 28 kVp W/Rh. The breast radius was 12 cm. The resulting DgN and DgN_V coefficients were then interpolated or extrapolated (on the basis of breast thickness and glandularity) to provide DgN and DgN_V coefficients based on the homogeneous breast model for each breast summarised in Table I. The resulting coefficients were then compared with those calculated for the same breasts using the corresponding voxelised anthropomorphic heterogeneous breast models.

In a second set of comparisons, the difference between dose estimates for the simple full homogeneous breast model and the full heterogeneous patient phantoms was evaluated again but with the size of the simple breast model individually matched by area to each patient phantom.

Sechopoulos *et al*¹⁵ and Hernandez *et al*²⁴ showed that when a realistic patient-based heterogeneous glandular tissue distribution is considered, the estimated breast dose is, on average, about 30% lower than that estimated for a breast defined as a homogeneous mixture of adipose and glandular tissue, with all other conditions being equal. In order to perform this same comparison but for spot mammography, the heterogeneous breast tissue within the patient specific spot heterogeneous breasts was substituted with homogeneous breast tissue of the corresponding overall glandular fraction (by mass) and the resulting DgN coefficients were compared.

In the case of the patient specific spot heterogeneous breasts, the position of the irradiated area, and therefore of the compression paddle, may influence the DgN coefficient due to the non-uniform glandular tissue distribution within the breast. To determine the sensitivity of MGD on spot compression position, one specific patient spot heterogeneous breast phantom was selected (glandular fraction by mass = 17%; breast thickness = 6.9 cm; breast area = 163 cm²) and was irradiated in seven different positions. These positions were obtained by laterally shifting the compression paddle (9 × 9 cm²), attached at the chest-wall, by 13.65 mm (50 voxels) per step.

2.G. D-shaped compression paddle

Some mammographic systems use a D-shaped compression paddle for spot compression. In this case, the field of view may extend beyond the compressed area, irradiating also the uncompressed breast portion. When the breast is entirely within the field of view, the mean glandular dose concept as defined in eq. 1 applies, requiring a different analysis than the one

proposed in the previous sections. For this, we also modelled the PMMA compression paddle with a circular shape with a radius of 7.5 cm and cutting a small segment with a chord length of 6.5 cm at the chest wall side. The paddle thickness was 0.2 cm. The compressed portion of the breast was defined by subtracting a $7.50 \times 5.65 \text{ cm}^2$ rectangular block from the full-field compressed breast. In simulations performed with this model, the source was located at 64.5 cm from the support paddle and electronically collimated in order to irradiate a $14 \times 30 \text{ cm}^2$ detector at 1 cm from the bottom breast surface, which meant that the breast was entirely in the field of view. The adopted spectrum was W/Rh at 28 kV.

Two simulations were repeated with this D-shaped compression paddle. First, we evaluated the effect of varying the uncompressed breast portion thickness on the DgN calculation for this new geometry. For this, we modelled a spot homogeneous breast phantom with a compressed thickness of 3 cm while the thickness of the uncompressed portion of the breast ranged between 3 cm (as adopted in full-field compression) and 7 cm. The breast radius was varied to maintain a constant total glandular tissue mass as the uncompressed breast portion was made thicker, starting from a 12 cm radius. The distance between the chest-wall and the compression paddle edge was set to 0 cm. Second, we analysed the influence of the distance from the chest to the compression paddle on the DgN and DgN_V estimates. This study was performed with a spot homogeneous breast with a compressed thickness of 3 cm and thickness of the uncompressed portion of 5 cm and 20% glandular fraction. The selected spectrum was W/Rh at 28 kV.

3. Results

3.A. Homogeneous model

3.A.1. Compression paddle area—Figure 4 shows the ratio between E_V and E_T for varying areas of the directly irradiated breast surface, ranging from 0.8 cm^2 (for a compression paddle of $1 \times 1 \text{ cm}^2$) to 226.2 cm^2 (for a full-field irradiation), for a 5 cm thick 20% glandular full homogeneous breast (28 kVp, W/Rh).

As expected, the ratio E_V/E_T monotonically increases up to 100% (i.e. the value for full-field irradiation) as the directly irradiated surface increases. For a compression paddle of $9 \times 9 \text{ cm}^2$ (directly irradiated area = 63.4 cm^2), about 95% of the energy absorbed in the breast glandular tissue is absorbed in the directly irradiated portion. DgN (fig. 5a) and DgN_V (fig. 5b) values increase as the area of the directly irradiated surface increases.

As expected, using the conventional definition for the glandular dose in spot compression mammography (MGD/DgN) leads to a substantially lower dose value compared to the case when only the directly irradiated part of the breast is taken into account (MGD_V/DgN_V) (fig. 6). Moreover, DgN_M values are lower compared to the other dose estimates defined in this work, at all energies investigated (fig. 6).

For monoenergetic x-ray beams (energy range 8–45 keV) and a $9 \times 9 \text{ cm}^2$ compression paddle, DgN_M and DgN are more than 60% lower than DgN_V (fig. 6). DgN_M coefficients, which approximate DgN in spot compression mammography, are between 3% and 14% lower compared to DgN in this photon energy range (fig. 6b). For W/Rh spectra at 28 kVp,

all three normalized glandular dose coefficients increase with increasing compression paddle area, up to the value for full-field irradiation, and are then the same in all cases (fig. 7). For a compression paddle area of $9 \times 9 \text{ cm}^2$, DgN_V is about 3 times higher than DgN and DgN_M . In the same conditions, DgN_M underestimates DgN by 6.7%. Decreasing the paddle area to $8 \times 8 \text{ cm}^2$ or $5 \times 5 \text{ cm}^2$ (paddle dimensions comprised in the range typically used in spot compression mammography) reduces DgN_V by 0.7% and 3.4%, respectively (fig. 7).

3.A.2. Effect of breast shape—Modeling the breast shape under spot compression more realistically, in which the compressed portion is thinner than the uncompressed portion, leads to results essentially the same as those obtained when the uncompressed and compressed regions of the breast are set to the same thickness. Figure 8 shows the three dosimetric parameters, for a 20% glandular breast and a breast thickness of 3 cm below the $9 \times 9 \text{ cm}^2$ compression paddle, for the spot homogeneous phantom. For a W/Rh spectrum at 28 kVp, all three normalized glandular dose coefficients depend weakly on the breast shape, as long as the total breast mass is constant. DgN_V for a 28 kVp W/Rh spectrum, remains almost constant, with only a 0.4% increase (MC statistical uncertainty = 0.2%) when increasing the thickness of the uncompressed breast portion from 3 to 7 cm.

As can be seen in Figure 9, DgN_V does not depend on the breast radius, and therefore on the overall breast mass, while DgN does. This is in contrast to the behavior of DgN in full-field mammography, where the dependence on breast diameter is considered negligible⁶ and a standard breast model with a standard diameter is adopted¹. For a 20% glandular spot homogeneous breast with a compressed thickness of 3 cm and an uncompressed thickness of 6 cm, increasing the breast radius from 9 cm to 12 cm (with the corresponding increase in the breast glandular mass) reduces DgN by 52%. In the same radius range, DgN_V remains constant apart from a small decrease between a breast radius of 9 cm (when the compression paddle is not entirely within the breast surface) and 10 cm.

3.A.3. Source-breast relative position—For a fixed distance between detector and source of 65.5 cm, DgN and DgN_V increase as the source to the breast support table distance increases and the magnification decreases (fig. 10). Reducing the source to the breast support table distance from 64.5 cm (i.e. spot compression without magnification) to 43.3 cm (i.e. spot magnification compression with $\times 1.5$ magnification factor) decreases DgN_V and DgN coefficients by 5.7% and 9.3% respectively, for a 20% glandular full homogeneous 5 cm breast and W/Rh spectrum at 28 kVp.

Increasing the distance from the irradiated portion of the breast to either the chest-wall (x-direction, fig. 11) or laterally to the center line of the breast (y-direction, fig. 12) has no influence on normalized glandular dose, unless a portion of the compression paddle extends beyond the breast surface. In this case, both DgN and DgN_M are reduced as the paddle and irradiated area extend further beyond the breast boundaries. Increasing the distance in the x-direction from 3 cm to 5 cm reduces DgN by 22% and DgN_M by 20%. A further increase to 7 cm reduces DgN and DgN_M by an additional 11% and 10%, respectively. Under these conditions, a weak increase can be observed in DgN_V of no more than 1.6%.

3.A.4. D-shaped compression paddles—Figure 13 shows the DgN coefficients for the D-shaped compression paddle as a function of the thickness of the uncompressed breast (W/Rh spectrum at 28 kVp). Differently from the case of partial breast irradiation (fig. 8), an increasing thickness of the uncompressed breast portion determines a large decrease of the calculated DgN coefficients. Modeling the uncompressed breast thickness of 7 cm instead of 3 cm reduced the DgN coefficient of 39%.

For the case of partial breast irradiation, in which the x-ray field is collimated to the spot compression paddle, increasing the distance between the compression paddle and the chest wall did not affect significantly the DgN and DgN_V. On the other hand, in the case in which the source is collimated to the entire detector, the larger the distance between the chest wall and the compression paddle, the smaller the area of the directly irradiated breast tissue (fig. 14). Therefore DgN decreases as the chest wall to the compression paddle distance increases (fig. 14). For a distance of 5 cm between chest wall and compression paddle, DgN is reduced by 57% compared to when the chest wall is in contact with the paddle and the breast is entirely in the field of view. A different trend can be observed for DgN_V, with a slight increase of 1.5% for the same 0 to 5 cm range (fig. 14).

3.B. Patient specific results

3.B.1 Validation of the voxelised Monte Carlo code—In the first validation test of the voxelised version of the MC code used in this work, the MGD per photon obtained with this code when assigning all voxels a homogeneous 20% glandular/80% adipose mixture was within -2.2% for the 16.8 keV monoenergetic x-ray beam and $+0.3\%$ for the 30 kVp Mo/Mo spectrum of the AAPM TG 195 Report results.

In the second validation, the comparison of a homogeneous breast defined as a simple solid to the voxelised version with random assignment of voxels as fully glandular or adipose (breast thickness = 5 cm; breast radius = 12 cm; glandularity = 20%; compression paddle = $9 \times 9 \text{ cm}^2$), resulted in differences in the normalized glandular dose coefficients lower than 2% for W/Rh spectra in the range 18–40 kVp (1.6% at 28 kVp). Similar results have been reported in the case of full-field breast irradiation²³.

For the second validation, the G factor is used for the homogeneous breast simulation but it is not used for the breast defined as randomly placed fully adipose and glandular voxels. Therefore, any differences in the mass energy absorption coefficients used for calculation of the G factor in the homogeneous case and the coefficients used internally by the MC code to simulate each interaction could introduce differences of this, albeit low, magnitude.

3.B.2 Patient specific normalized glandular dose coefficients—Figure 15 shows average DgN_V and DgN values obtained for the 20 patient specific spot heterogeneous breasts summarized in Table 1 evaluated for a compression paddle of $9 \times 9 \text{ cm}^2$ with different thicknesses for the uncompressed breast areas. As found for the homogeneous model, the results for each patient specific breast show that the normalized glandular dose coefficients do not vary with the shape of the uncompressed portion of the breast. Therefore, for both simple breast models and for realistic patient breasts, an accurate representation of

the relationship between the spot compressed and uncompressed areas of the breast is not needed for dosimetry evaluation.

By comparing the results in Fig. 15 to those in Fig. 8, it can be seen that the ratio between DgN and DgN_V is different for patient-specific heterogeneous breasts compared to that of the simple homogeneous breast model. In the patient breasts, the glandular tissue tends to be located towards the center of the breast. The spot being simulated for the results in Fig. 16 was located close to the center of the breast area, so a higher proportion of the glandular tissue was included within the directly irradiated volume, and most of the energy absorbed outside this volume was in adipose tissue. Therefore, in the case of the patient breasts the denominator in the calculation of MGD and MGD_V does not vary as much as in the case of the simple model, in which the distribution of glandular tissue is uniform across the whole breast.

Figure 16 shows the ratio between the DgN coefficients for spot compression when only the spot compressed area is irradiated to those when the entire breast is irradiated (irradiated area at the detector = $14 \times 30 \text{ cm}^2$). As already shown for the homogeneous breast model (fig. 7), in the case of partial irradiation the DgN coefficients are lower than those in full-field irradiation. The ratios are on average 0.66, 0.70 and 0.72 when the uncompressed breast portion is 60%, 80% and 100% of the thickness of the breast undergoing full-field examination, respectively.

DgN and DgN_V were estimated with an irradiated area matching the compression paddle of area $9 \times 9 \text{ cm}^2$ for each of the patient-based full heterogeneous breasts summarized in Table 1 and compared to the corresponding coefficients evaluated for the full homogeneous model for matching thicknesses and glandular fractions, but with a standardized breast radius of 12 cm and skin thickness of 0.4 cm. Figure 17 shows this comparison. The ratios for DgN and DgN_V are (mean \pm 1 SD) 0.54 ± 0.18 and 0.96 ± 0.19 , respectively. Therefore, using a simple full compressed homogeneous breast model with standardized size and skin thickness underestimates the MGD to patient breasts by about 50%. In addition to the expected influence of using a different skin thickness, the influence of breast area (Fig. 9) and the spatial distribution of the glandular tissue on DgN in spot mammography introduce important variations that would need to be addressed in future dosimetric breast models for spot mammography.

To confirm the effect of mismatched breast sizes causing, at least partially, the difference in DgN between patient breast dose estimates and that of the model, the simulations were repeated with the breast area of the full homogeneous model matched in turn to the breast areas of the corresponding patient specific full heterogeneous phantoms. In this case, as can be seen in Fig. 18, the mean ratio of DgN coefficients obtained with the customized homogeneous model and those obtained with the full heterogeneous breast increased to 0.91 (1 SD = 0.16).

Finally, figure 19 shows the ratio of DgN coefficients for the 20 patient phantoms when filled with an internal homogeneous tissue distribution vs. their actual heterogeneous glandular/adipose tissue distribution, as studied by Sechopoulos *et al*¹⁵ and Hernandez *et*

a^{24} for full field mammography. The ratio determined for spot mammography is, on average, 1.15 with a standard deviation of 0.20. Although this result is similar to those of Sechopoulos *et al*¹⁵ and Hernandez *et al*²⁴, in which they found an average difference of 1.30, the discrepancy can be explained by the influence of the irradiation position on the DgN coefficients evaluated for the full heterogeneous breast phantoms (fig. 20) as well as by the used spectra. Shifting the irradiation area by about 1.4 cm (from position 1 to position 2 in fig. 20a), the MGD to the breast increases by 10% for the full heterogeneous breast phantom. In both positions the irradiated area is entirely enclosed within the breast area. The MGD estimated for position 5 (fig. 20d), where a portion of the compression paddle is not within the compressed breast area, is 32% lower than that at position 3 (fig. 20c), in which the compression paddle is entirely within the breast area. The patient specific phantom used in this test is the one which produced the lowest values in figs. 17–19.

4. Discussion

The metrics used for radiation dosimetry in medical imaging should correlate with the risk associated with the use of ionizing radiation during acquisition. Currently accepted risk models are based on the absorbed dose to the entire organ of interest. In breast dosimetry it is considered that the tissue at highest risk of developing breast cancer is the glandular tissue, so the accepted dose metric in mammography is the glandular absorbed dose. Therefore, currently breast dosimetry is based on the mean glandular dose (MGD) to the entire breast, which is estimated using DgN and the incident air kerma.

This study has characterized how DgN behaves under various different imaging conditions and varied breast models during spot compression mammography. Due to the partial breast irradiation nature of this modality in some systems, the characteristics of DgN change somewhat compared to full-field imaging. For example, in this modality DgN does vary considerably with breast size, a factor which is usually considered to not affect DgN in full field mammography. Therefore, assumptions and simplifications in the breast model that include a specific breast area can introduce a larger bias in the dose estimates that might be present in the dosimetry models for full field mammography. It was also found that, by employing a homogeneous breast model as used in full field mammography, as long as the directly irradiated portion does not extend beyond the edges of the breast, DgN does not vary considerably with the position of the irradiated area. This is different for the case in which a breast with a real shape and a heterogeneous glandular distribution, in which the DgN can vary, even though the field of view is comprised within the breast area. More surprisingly perhaps, the relation between the thicknesses of the compressed and uncompressed portions of the breast does not affect DgN, in the case in which only the compressed area is directly irradiated. Considering the potential difficulties in modelling this difference in thickness, this is a welcome finding. On the other hand, the thickness of the uncompressed breast does influence the DgN coefficient if the beam is not collimated to the compression paddle dimensions. Overall, care must be taken in defining a simplified breast model undergoing spot compression mammography, especially under the partial breast irradiation condition, that does not introduce important biases in the estimates due to inappropriate assumptions in breast size and glandular tissue distribution.

The aim of this work was to obtain insights into the variation in dose estimates for spot compression mammography as breast model and image acquisition conditions are varied. This characterization will be useful in the development of a new breast dosimetry model for mammography and breast tomosynthesis imaging, which will include the dosimetry of common non-screening views, a task currently being undertaken by a joint task group of the AAPM²⁵ and the EFOMP.

Considering the large variation in *local* dose deposition throughout the breast due to the use of relatively low x-ray energies^{26,27}, it could be debated if averaging the glandular dose over the entire breast is really the most appropriate risk-related metric for full field mammography. In a related fashion, the results for DgN_V show that this might also be a valid discussion point for imaging that involves partial field irradiation of the breast. The use of the mean dose to the whole breast means that during acquisition of a spot compression image, the risk is lowered if the breast is larger even when the extra tissue is located well beyond the field of view. Although the appropriateness of the current risk model is beyond the scope of this work, the insight gained here on DgN_V might be useful in the future if the local variations in dose during breast imaging become part of the accepted dosimetry model. The metric DgN_M , proposed to avoid the need for new MC simulations and tables of data, was found to underestimate dose by up to 14% for monoenergetic photons at 45 keV, although such underestimation reduces with photon energy and is 6.7% for a W/Rh spectrum at 28 kVp. Therefore, until new results are available, the use of DgN_M can provide an adequate estimate of the mean glandular dose.

5. Conclusions

The behaviour of DgN in spot compression mammography for different breast models and acquisition parameters was characterized in preparation for a new breast dosimetry model being undertaken by a newly formed task group. The DgN_M provides reasonable estimates of DgN for spot compression without the need for new simulations or tables typically to within 7%. Finally, an alternative metric, DgN_V , which considers only the local dose to the area of the breast being directly irradiated, might be useful in the future if local dose deposition levels are considered relevant in the accepted risk models.

Acknowledgments

Work supported in part by grants CA163746 (IS), CA181171 (IS), CA176684 (BF) and CA156775 (BF) from the National Cancer Institute, National Institutes of Health, and IIR13262248 (IS) from the Susan G. Komen Foundation. This work was supported in part by the MaXIMA project H2020-TWINN-2015 (grant no. 692097) (KB, PR, GM, AS, FDL), and by the INFN (AS, PR, GM, FDL). The content is solely the responsibility of the authors and does not necessarily represent the official views of the National Cancer Institute, the National Institutes of Health, the Susan G. Komen Foundation or the INFN. The contribution of DRD was funded as part of the OPTIMAM2 project which is funded by Cancer Research UK (grant number: C30682/A17321). KCY works for the National Coordinating Centre for the Physics of Mammography funded by Public Health England.

References

1. Dance DR. Monte Carlo calculation of conversion factors for the estimation of mean glandular breast dose. *Phys Med Biol.* 1990; 35:1211–1219. [PubMed: 2236205]
2. Wu X, Gary TB, Tucker DM. Spectral dependence of glandular tissue dose in screen-film mammography. *Radiology.* 1991; 179:143–148. [PubMed: 2006265]

3. Wu X, Gingold EL, Barnes GT, Tucker DM. Normalized average glandular dose in molybdenum target-rhodium filter and rhodium target-rhodium filter mammography. *Radiology*. 1994; 193:83–89. [PubMed: 8090926]
4. Boone JM. Glandular breast dose for monoenergetic and high-energy x-ray beams: Monte Carlo assessment. *Radiology*. 1999; 213:23–37. [PubMed: 10540637]
5. Dance DR, Skinner CL, Young KC, Beckett JR, Kotre CJ. Additional factors for the estimation of mean glandular breast dose using UK mammography dosimetry protocol. *Phys Med Biol*. 2000; 45:3225–3240. [PubMed: 11098900]
6. Boone JM. Normalized glandular dose (DgN) coefficients for arbitrary x-ray spectra in mammography: Computer-fit values of Monte Carlo derived data. *Med Phys*. 2002; 29:869–875. [PubMed: 12033583]
7. Dance DR, Young KC, van Engen RE. Further factors for the estimation of mean glandular breast dose using United Kingdom, European and IAEA breast dosimetry protocols. *Phys Med Biol*. 2009; 54:4361–4372. [PubMed: 19550001]
8. Dance DR, Young KC. Estimation of mean glandular dose for contrast enhanced digital mammography: factors for use with the UK, European and IAEA breast dosimetry protocols. *Phys Med Biol*. 2014; 59:2127–2137. [PubMed: 24699200]
9. Nosratieh A, Hernandez A, Shen SZ, Yaffe MJ, Seibert JA, Boone JM. Mean glandular dose coefficients (DgN) for x-ray spectra used in contemporary breast imaging systems. *Phys Med Biol*. 2015; 60:7179–7190. [PubMed: 26348995]
10. Mettivier G, Fedon C, Di Lillo F, Longo R, Sarno A, Tromba G, Russo P. Glandular dose in synchrotron radiation breast computed tomography. *Phys Med Biol*. 2016; 61:569–587. [PubMed: 26683710]
11. Liu B, Goodsitt M, Chan HP. Normalized average glandular dose in magnification mammography. *Radiology*. 1995; 197:27–32. [PubMed: 7568836]
12. Koutaloni M, Delis H, Spyrou G, Costaridou L, Tzanakos G, Panayiotakis G. Monte Carlo generated conversion factors for the estimation of average glandular dose in contact and magnification mammography. *Phys Med Biol*. 2006; 51:5539–5548. [PubMed: 17047268]
13. Institute of Physics and Engineering in Medicine (IPEM). IPEM Report. Vol. 89. York, United Kingdom: IPEM; 2005. The commissioning and routine testing of mammographic X-ray systems.
14. Hammerstein RG, Miller DW, White DR, Masterson ME, Woodard HQ, Laughlin JS. Absorbed radiation dose in mammography. *Radiology*. 1979; 130:485–491. [PubMed: 760167]
15. Sechopoulos I, Bliznakova K, Qin X, Fei B, Feng SSJ. Characterization of the homogeneous tissue mixture approximation in breast imaging dosimetry. *Med Phys*. 2012; 39:5050–5059. [PubMed: 22894430]
16. Yang X, Wu S, Sechopoulos I, Fei B. Cupping artifact correction and automated classification for high-resolution dedicated breast CT images. *Med Phys*. 2012; 39:6397–6406. [PubMed: 23039675]
17. Zyganitidis C, Bliznakova K, Pallikarakis N. A novel simulation algorithm for soft tissue compression. *Med Biol Eng Comp*. 2007; 45:661–669.
18. Sechopoulos I, Suryanarayanan S, Vedantham S, D'Orsi CJ, Karellas A. Computation of the glandular radiation dose in digital tomosynthesis of the breast. *Med Phys*. 2007; 34:221–232. [PubMed: 17278508]
19. Fedon C, Longo F, Mettivier G, Longo R. GEANT4 for breast dosimetry: parameters optimization study. *Phys Med Biol*. 2015; 60:N311–N323. [PubMed: 26267405]
20. Hubbell, JH., Seltzer, SM. [accessed on 05-23-2016] Tables of X-Ray Mass Attenuation Coefficients and Mass Energy Absorption Coefficients from 1 keV to 20 MeV for Elements Z = 1 to 92 and 48 Additional Substances of Dosimetric Interest available. 2004. from <http://www.nist.gov/pml/data/xraycoef/index.cfm>
21. Hernandez AM, Boone JM. Tungsten anode spectral model using interpolating cubic splines: Unfiltered x-ray spectra from 20 kV to 640 kV. *Med Phys*. 2014; 41:042101-1–15. [PubMed: 24694149]
22. Sechopoulos I, Ali ES, Badal A, Badano A, Boone JM, Kyprianou IS, Mainegra-Hing E, McMillan KL, McNitt-Gray MF, Rogers DWO, Samei E, Turner AC. Monte Carlo reference data sets for

- imaging research: Executive summary of the report of AAPM Research Committee Task Group 195. *Med Phys.* 2015; 42:5679–5691. [PubMed: 26429242]
23. Sarno A, Mettivier G, Di Lillo F, Russo P. A Monte Carlo study of monoenergetic and polyenergetic normalized glandular dose (DgN) coefficients in mammography. *Phys Med Biol.* 2017; 62:306–325. [PubMed: 27991451]
24. Hernandez MA, Seibert JA, Boone JM. Breast dose in mammography is about 30% lower when realistic heterogeneous glandular distributions are considered. *Med Phys.* 2015; 42:6337–6348. [PubMed: 26520725]
25. [accessed on 10-19-2016] American Association of Physicists in Medicine - website. http://www.aapm.org/org/structure/default.asp?committee_code=TG282
26. Thacker SC, Glick SJ. Normalized glandular dose (DgN) coefficients for flat-panel CT breast imaging. *Phys Med Biol.* 2004; 49:5433–5444. [PubMed: 15724534]
27. Sechopoulos I, Feng SSJ, D’Orsi CJ. Dosimetric characterization of a dedicated breast computed tomography clinical prototype. *Med Phys.* 2010; 37:4110–4120.

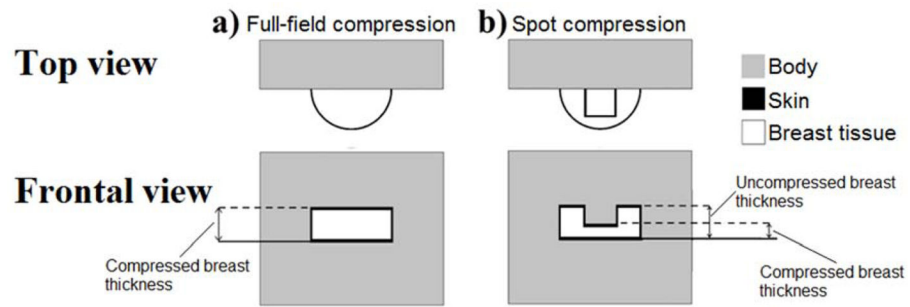


Fig. 1.
Schematic of the homogeneous breast model in a) full-field compression (denoted the full homogeneous phantom) and in b) spot compression (spot homogeneous phantom).

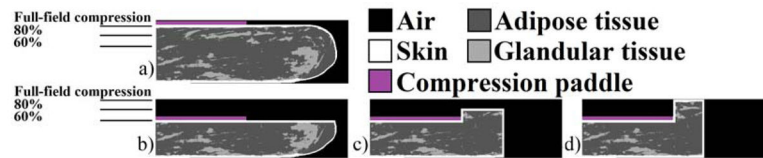


Fig. 2.

Sagittal slice of one patient specific breast phantom (a) under full-field compression (the full heterogeneous phantom), and under spot compression (the spot heterogeneous phantom) to 60% of the thickness of the full-field case and with the uncompressed portion having a thickness of (b) 60%, (c) 80% and (d) 100% of the full-field case.

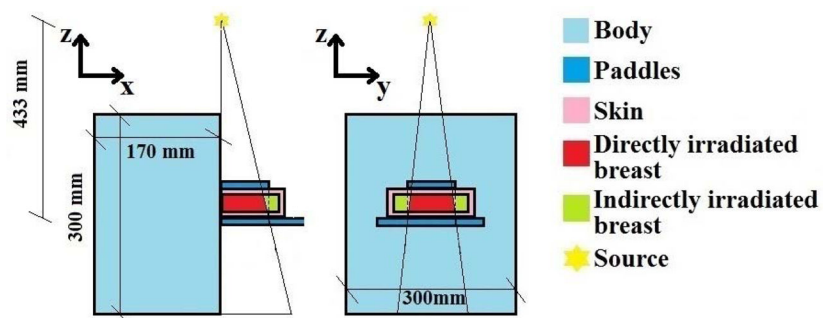


Fig. 3.

Irradiation geometry used in this work. The isotropic point source is located 43.3 cm from the breast support table and the x-ray beam is collimated in order to directly irradiate an area on the support table as large as the compression paddle.

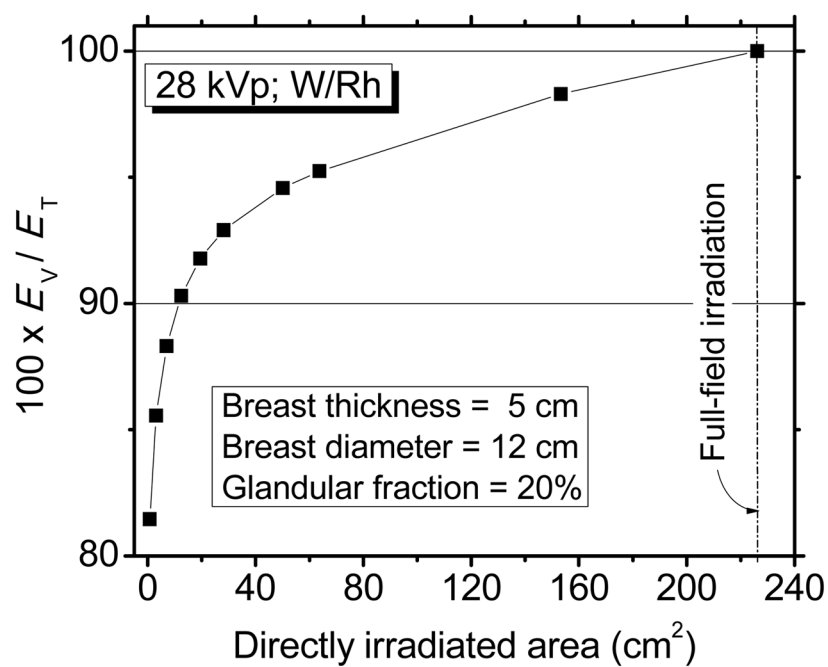


Fig. 4.

Percent ratio between E_V and E_T for an irradiated area ranging between 0.8 cm² and 226.2 cm² (full-field irradiation) for the full homogeneous breast phantom.

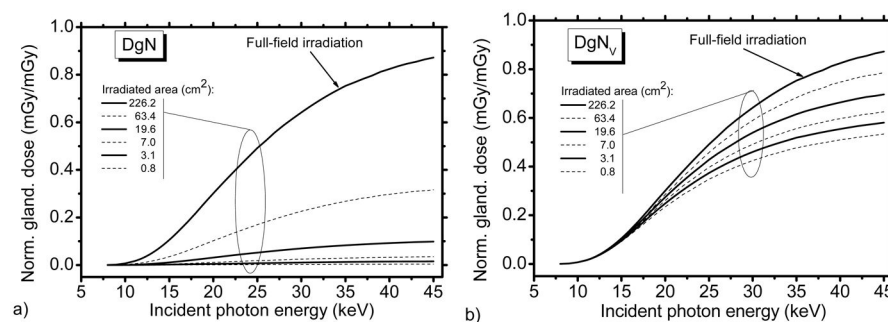


Fig. 5. Monoenergetic (a) DgN and (b) DgN_V for a 20% glandular full homogeneous breast phantom with a thickness of 5 cm.

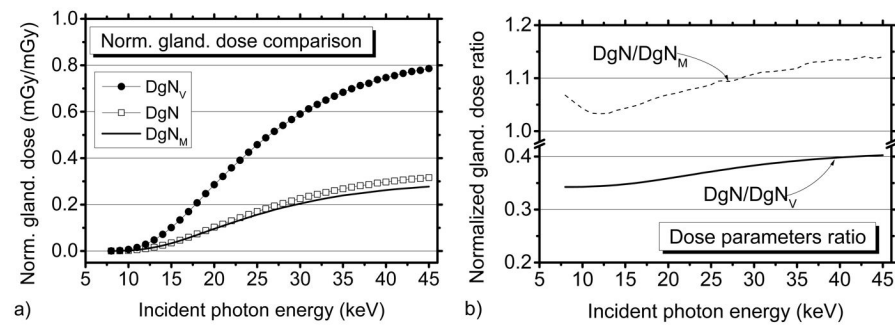
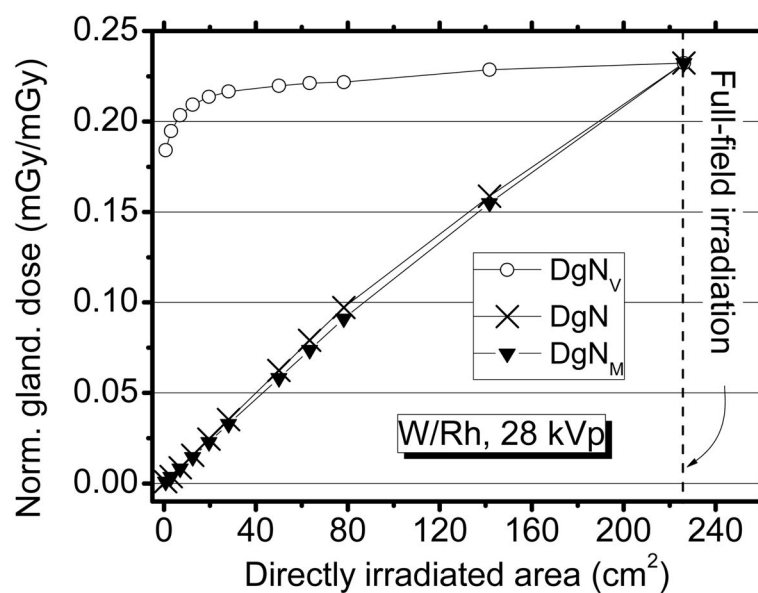


Fig. 6.

a) Comparison of the three DgN conversion coefficients for a single full homogeneous breast and compression paddle size and their variation with monoenergetic x-ray energy. b) DgN/DgN_M and DgN/DgN_V ratio. Breast thickness = 5 cm; glandular fraction = 20%; compression paddle area = $9 \times 9 \text{ cm}^2$.

**Fig. 7.**

Polyenergetic DgN, DgN_V and DgN_M for a 20% glandular breast with a thickness of 5 cm (constant thickness compression) for varying compression paddle size.

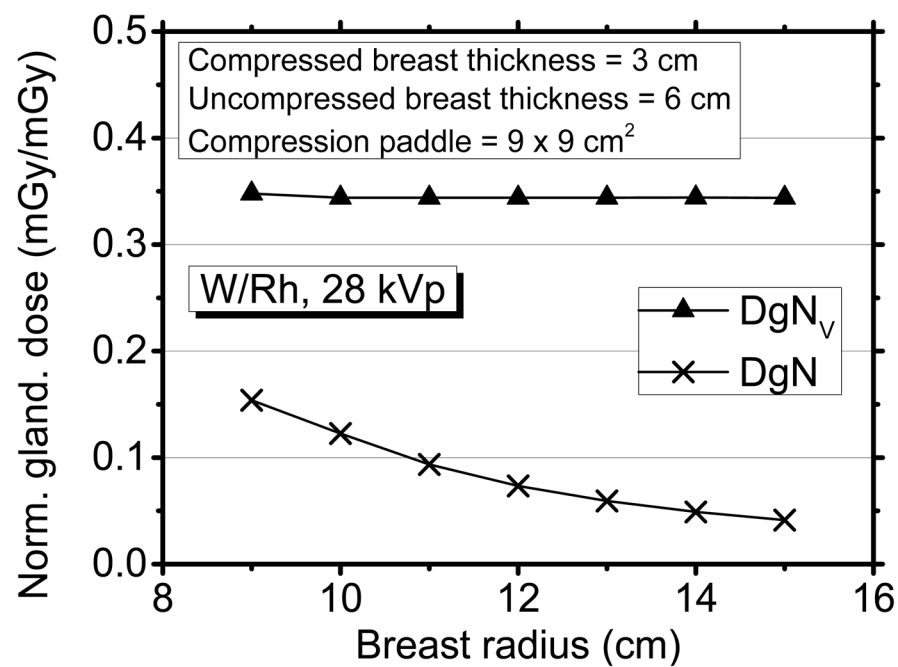


Fig. 8.

Polyenergetic DgN , DgN_V and DgN_M for a 20% glandular spot homogeneous breast. Breast thickness between the paddles = 3 cm; compression paddle = 9 × 9 cm².

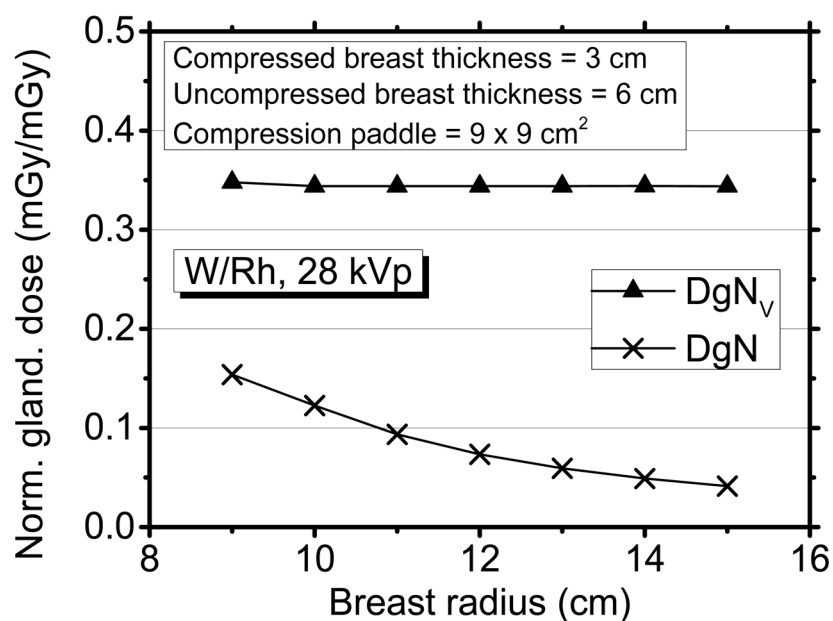
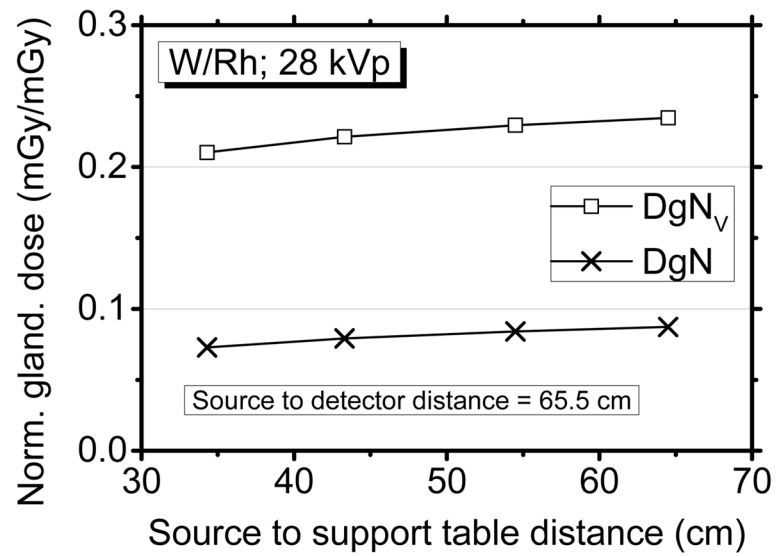


Fig. 9.
Polyenergetic DgN and DgN_v for a 20% glandular spot homogeneous breast with varying breast radius.

**Fig. 10.**

Polyenergetic DgN and DgN_v at different source to breast support table distances. Full homogeneous breast with thickness = 5 cm; glandular fraction = 20%, breast radius = 12 cm, compression paddle area = $9 \times 9 \text{ cm}^2$.

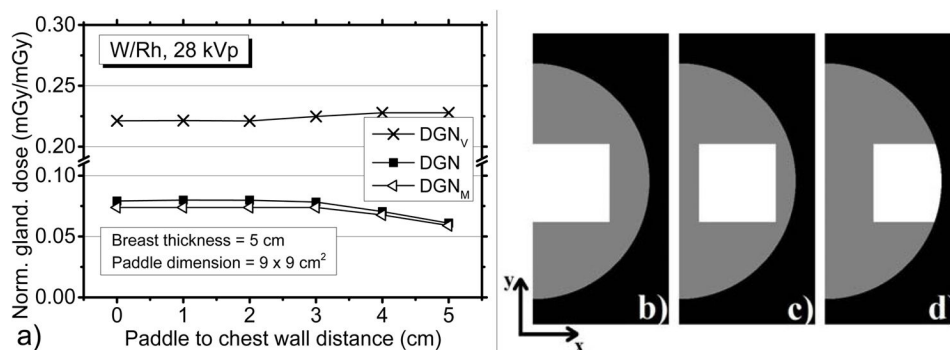


Fig. 11.

a) Polyenergetic DgN , DgN_V and DgN_M at different compression paddle – to – chest wall distances. Full homogeneous breast phantom, with glandular fraction = 20%, breast radius = 12 cm. Drawing of the modeled breast, in grey, with the direct irradiated area in white for distances between chest wall and compression paddle of (b) 0 cm, (c) 2 cm and (d) 5 cm.

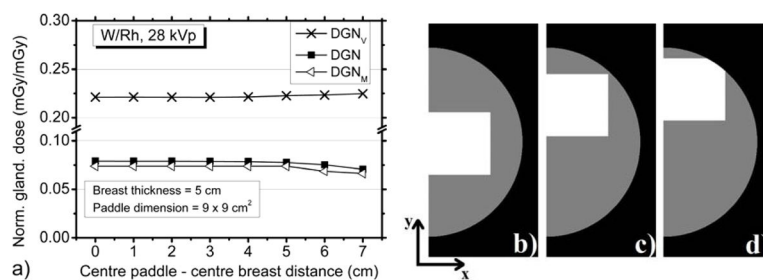


Fig. 12.

Polyenergetic DgN , DgN_V and DgN_M at different compression paddle center – breast center distances. Full homogeneous breast phantom, glandular fraction = 20%, breast radius = 12 cm. Drawing of the modeled breast, in grey, with the directly irradiated area in white for distances between the centre of the paddle and the centre of the breast of (b) 0 cm, (c) 5 cm and (d) 7 cm.

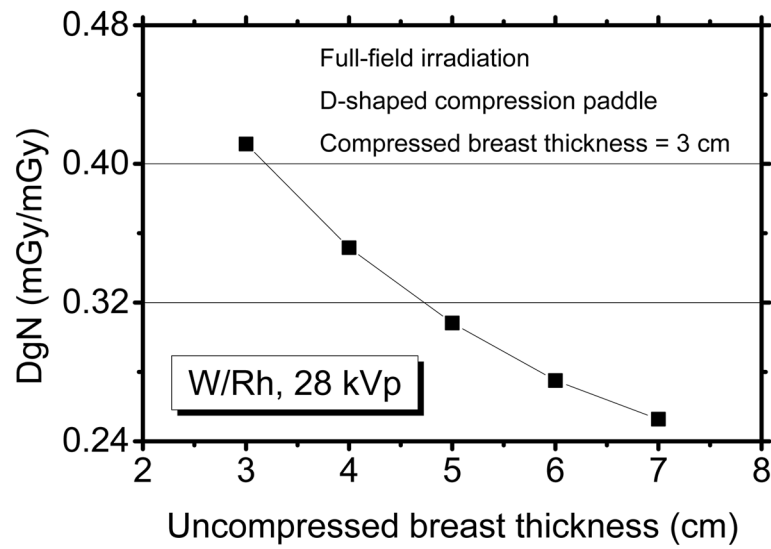


Fig. 13. Polyenergetic DgN as a function of the thickness of the uncompressed portion of the breast, when the compressed breast thickness is fixed at 3 cm for a 20% glandular breast.

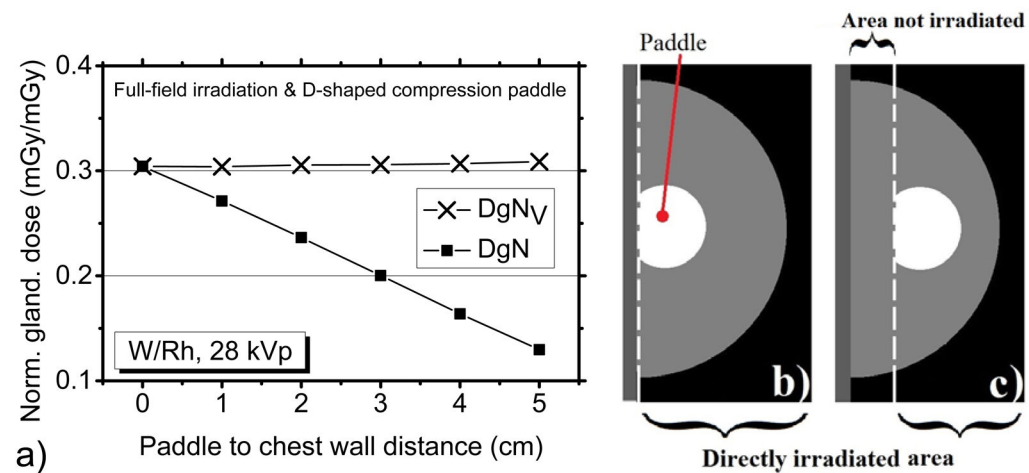


Fig. 14.

a) Polyenergetic DgN and DgN_V as a function of compression paddle-to-chest wall distance for a 12 cm radius, 20% glandular breast compressed with a D-shaped paddle to 3 cm and an uncompressed breast portion 5 cm thick. The irradiation geometry is illustrated in b) and c) for the case of zero distance and 2 cm distance between chest wall and compression paddle, respectively. Only the part of the breast to the right of the dashed line is irradiated directly.

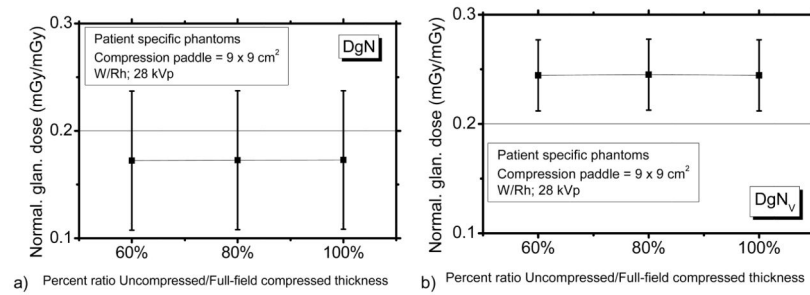


Fig. 15.

Average of the polyenergetic a) DgN and b) DgN_V results for the 20 patient specific breasts summarized in Table 1 for a compressed breast thickness between the paddles of 60% of the full-field compressed breast thickness. The error bars were evaluated as the standard deviation of the results obtained for the 20 patient breasts.

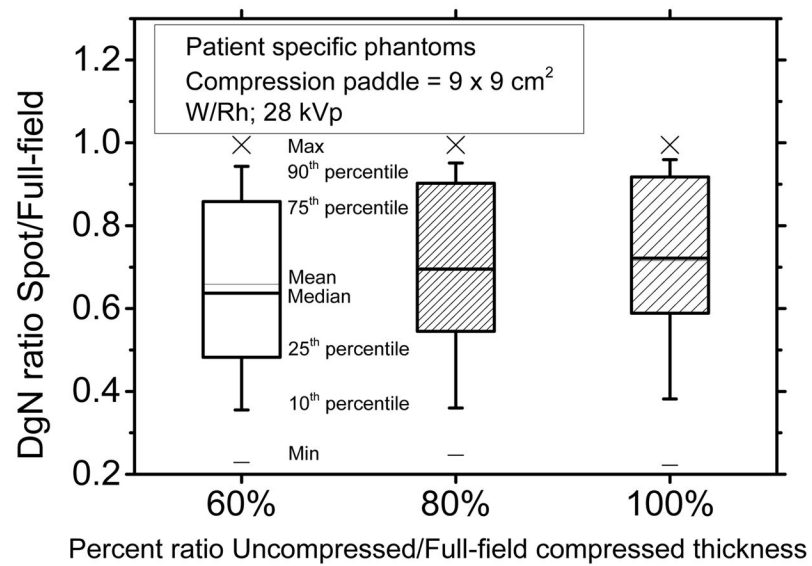


Fig. 16.

Box-whisker plot of the ratio between the polyenergetic DgN coefficients evaluated in the case of partial and full field irradiation when the breast is under spot compression for the specific breasts indicated in Table 1. The thickness of the spot compressed portion of the breast is 60% of the full-field compressed breast. The mean and median bars for the 80% and 100% ratios overlap.

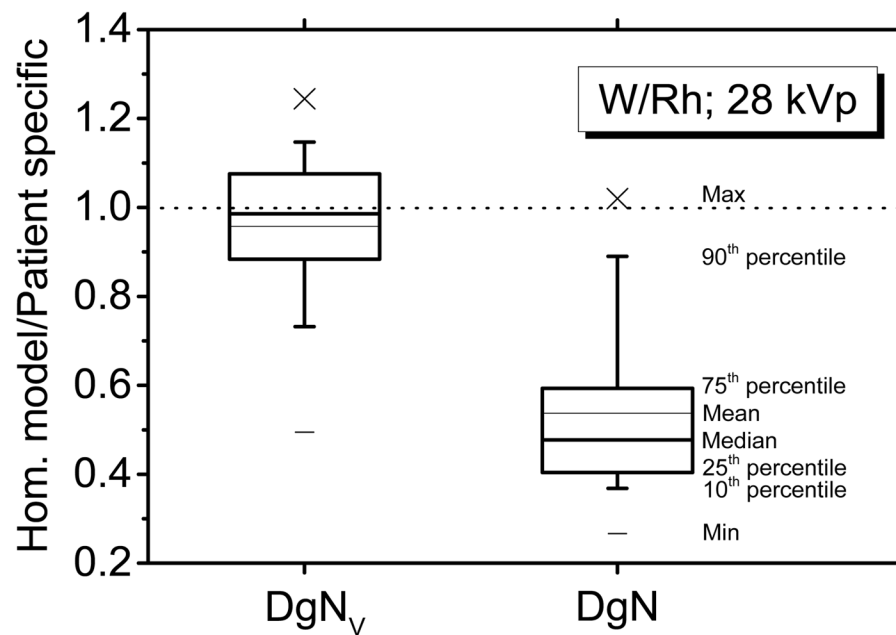
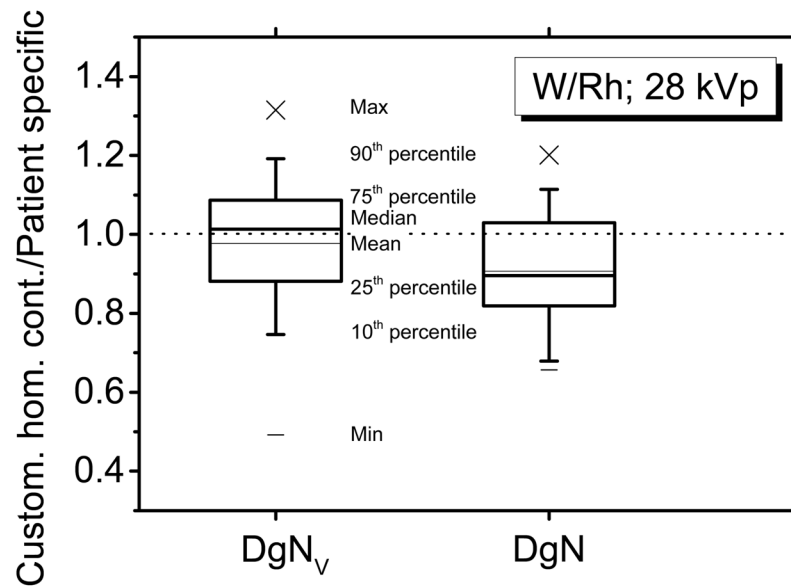


Fig. 17.

Box-whisker plot of the ratio between the normalized glandular dose obtained with the full homogeneous breast model (skin thickness = 0.4 cm; breast radius = 12 cm) and that obtained with the full heterogeneous patient specific breast phantom. W/Rh spectrum at 28 kVp, compression paddle dimension = $9 \times 9 \text{ cm}^2$; $\times 1.5$ magnification.

**Fig. 18.**

Box-whisker plot of the ratio between the normalized glandular dose obtained with the customized full homogeneous breast model (skin thickness = 0.4 cm) and that obtained with the patient specific full heterogeneous breast phantoms. The breast areas and glandularities were matched for each corresponding patient specific breast phantom. W/Rh spectrum at 28 kVp, compression paddle dimension = $9 \times 9 \text{ cm}^2$; $\times 1.5$ magnification.

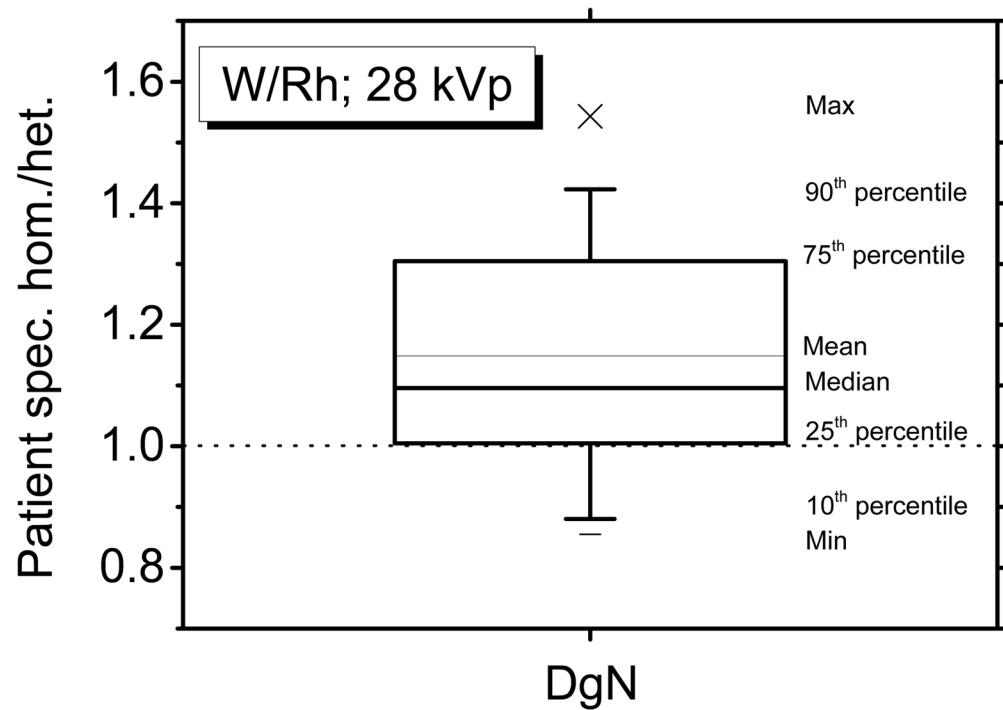


Fig. 19.

Box-whisker plot of the ratio between the normalized glandular dose obtained with the homogeneous patient specific breast phantom and that obtained with the original heterogeneous version. W/Rh spectrum at 28 kVp, compression paddle dimension = 9×9 cm²; $\times 1.5$ magnification.

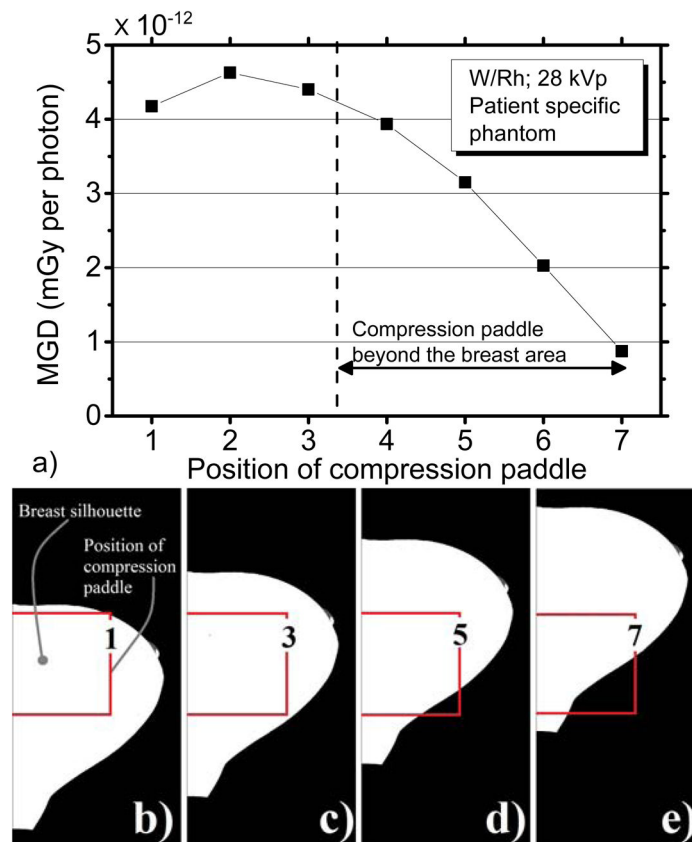


Fig. 20.

a) MGD per generated photon, for different locations of the compression paddle for the full heterogeneous phantom. The numbers 1, 3, 5, 7 in b)–e) identify the position of the compression paddle (outlined in red) in the field of view. W/Rh spectrum at 28 kVp, compression paddle dimension = $9 \times 9 \text{ cm}^2$; $\times 1.5$ magnification.

Table I

Characteristics of the 20 patient specific full heterogeneous phantoms used in the “fully-compressed” spot dosimetry simulations, as shown in Fig. 2(a).

	Mean	Stand. Dev.	Min	Max
Compressed thickness (cm)	5.9	1.5	2.9	7.8
Area (cm ²)	123.79	54.85	31.11	250.90
Glandular fraction by mass (%)	23.1	15.4	5.0	54.3